Electronic Supplementary Information (ESI)

Synthesis of FeP_2/C nanohybrids and their performance for hydrogen evolution reaction

Jun Jiang, [a,b,c,d] Chunde Wang,[a,b,c,d] Jiajia Zhang,[a,e] Wenliang Wang,[a,b,c,d] Xiaoli Zhou,[a,b,c,d] Bicai Pan,[a,e] Kaibin Tang,[a,b] Jian Zuo,[a] Qing Yang*,[a,b,c,d]

[a] Hefei National Laboratory of Physical Sciences at the Microscale, University of Science and Technology of China (USTC), Hefei 230026, Anhui, P. R. China.

[b] Department of Chemistry, USTC, Hefei 230026, Anhui, P. R. China.

[c] Laboratory of Nanomaterials for Energy Conversion, USTC, Hefei 230026, Anhui, P. R. China.

[d] Synergetic Innovation Center of Quantum Information & Quantum Physics, USTC, Hefei 230026, Anhui, P. R. China.

[e] Department of Physics, USTC, Hefei 230026, Anhui, P. R. China.

* Corresponding author. E-mail: qyoung@ustc.edu.cn; Fax: +86-551-63606266; Tel: +86-551-63600243.

1. Experimental

Materials. Ferrocene ($Fe(C_5H_5)_2 \geq 95\%$) is purchased from Alfa Aesar. Red phosphorus (powder, 99% purity), selenium powder (99% purity) and solvent of ethanol are all obtained from Shanghai Chemical Reagents Company, China. All reagents are used as received without further purification.

Synthesis of FeP_2/C nanohybrids. Synthetic procedures to the FeP_2/C nanohybrids are adopted from our previous work[S1] performed in an evacuated and sealed quartz tube with variations of precursors and reaction temperatures, and the details are described as below. In a typical synthesis, a mixture of 0.112 g (~0.6 mmol) of $Fe(C_5H_5)_2$ and 0.038 g (~1.2 mmol) of red phosphorus is tableted and put into a quartz tube (φ8 mm × 150 mm), which is then evacuated and sealed. The tube is loaded into a resistance furnace horizontally, heated from room temperature to 500 °C at a rate of 2 °C min^{-1}, and kept at this reaction temperature for 30 h. After reaction the tube is naturally cooled to room temperature, black products are collected, washed with absolute alcohol several times, and finally dried in a vacuum furnace at 60 °C for further investigation.

Structure Characterization. The purity and phases of the products are identified by X-ray diffraction (XRD) patterns on a Philips X'Pert Pro Super diffractometer with graphite-monochromatized Cu-Ka radiation (λ = 1.54178 Å). The morphologies of the product are examined by field emission scanning electron microscope (SEM, JEOL JSM-6700F). The high resolution TEM (HRTEM), selected area electron diffraction (SAED) patterns, high-angle annular dark-field scanning transmission electron microscope (HAADF-STEM) and corresponding energy-dispersive X-ray spectroscope (EDX) mapping analyses are performed on a JEOL JEM-ARF200F TEM/STEM with a spherical aberration corrector. Raman spectrum is carried out on a JY LABRAM-HR confocal laser micro-Raman spectrometer using Ar^+ laser excitation with a wavelength of 514.5 nm. The weight percentage of carbon and hydrogen are characterized by elemental analysis (EA, Elemental vario EL cube, Thermal Conductivity Detector) at pure oxygen atmosphere. The surface structures of the samples are determined by attenuated total reflection Fourier transformed infrared (ATR-FTIR) spectroscopy (Prestige-21, SHIMADZU). X-ray photoelectron spectra (XPS) are acquired on an ESCALAB MK II with Mg Kα as the excitation source. The BET (Brunauer–Emmett–Teller) surface area and BJH (Barrett–Joyner–Halenda) porous distribution plots are measured on a Micromeritics ASAP 2020 accelerated surface area and porosimetry system.

Electrochemical Characterization. All the electrochemical measurements are conducted in a typical three-electrode setup with an electrolyte solution of 0.50 M H_2SO_4, a Ag/AgCl (in saturated KCl solution) electrode as the reference electrode, a graphite rod as the counter electrode. The preparation of working electrodes is

described as below. Typically, 6 mg of catalyst and 40 μL of Nafion solution (Sigma Aldrich, 5 wt%) are dispersed in 1 mL water-ethanol solution with volume ratio of 4:1 by sonicating for several hours to form a homogeneous ink. Then 5 μL of the catalyst ink (containing 30 μg of catalyst) is loaded onto a glassy carbon electrode of 3 mm in diameter (loading ~ 0.425 mg cm^{-2}). Finally, the as-prepared working electrode is dried at room temperature. The working electrodes of bulk FeP_2 and Pt/C (20 wt.%) with the same mass loading are also prepared. All of the potentials in our manuscript are calibrated to a reversible hydrogen electrode (RHE) based on the Nernst equation. Polarization curves are obtained by linear sweep voltammetry with a scan rate of 5 mV s^{-1} while rapidly stirring the solution with a magnetic stir bar and continually bubbling the electrolyte solution with high purity hydrogen. Cyclic voltammetry (CV) is conducted between −0.2 and 0.2 V vs RHE at a scan rate of 100 mV s^{-1}. The electrochemistry impedance spectrum (EIS) is measured in an electrochemical workstation (CHI660E) with the frequency from 100 KHz to 0.01 Hz at an overpotential of 200 mV.

2. Nitrogen adsorption-desorption isotherms of the FeP_2/C nanohybrids

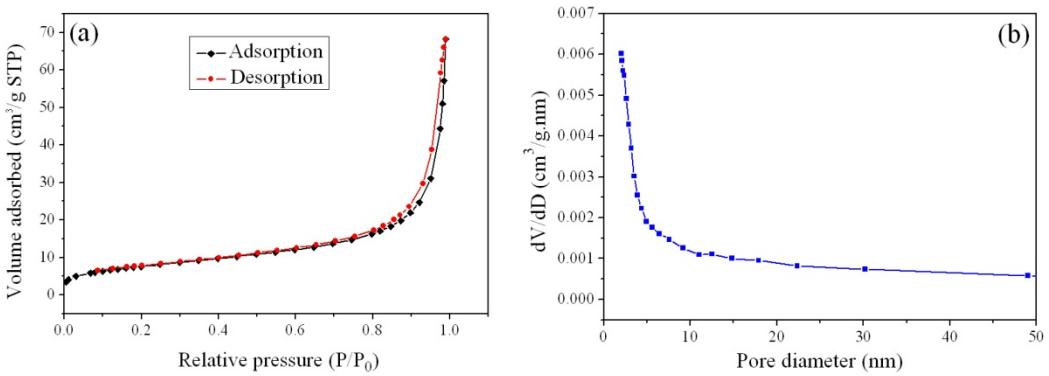

Fig. S1. Nitrogen sorption isothermals and the corresponding pore size distribution curve of the FeP_2/C nanohybrids. The BET surface area, mean pore size, and pore volume derived from the adsorption branch are 27.7 m^2 g^{-1}, 15.7 nm, and 0.1 cm^3 g^{-1}, respectively.

3. EDX spectra of the FeP_2/C nanohybrids

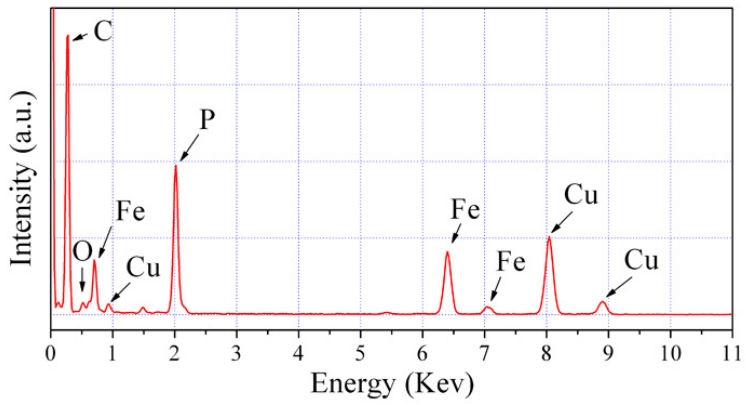

Fig. S2. EDX spectra of the FeP_2/C nanohybrids. The signal of Cu arises from the

TEM grid.

4. Synthesis of bulk FeP_2 with their XRD pattern and SEM images

Synthesis of bulk FeP_2. Synthetic procedures to the bulk FeP_2 are adopted from previous work.[S2] In a typical synthesis, Fe powder (1 mmol, 0.056g) and red phosphorus (2 mmol, 0.062g) are tableted and put into a quartz tube (φ8mm × 150 mm), which is then evacuated and sealed. The tube is loaded into a resistance furnace horizontally, heated from room temperature to 700 °C at a rate of 2 °C/min, and kept at this reaction temperature for 5 day. After that, they are cooled to room temperature via quenching in water and then the black products are collected for further characterizations.

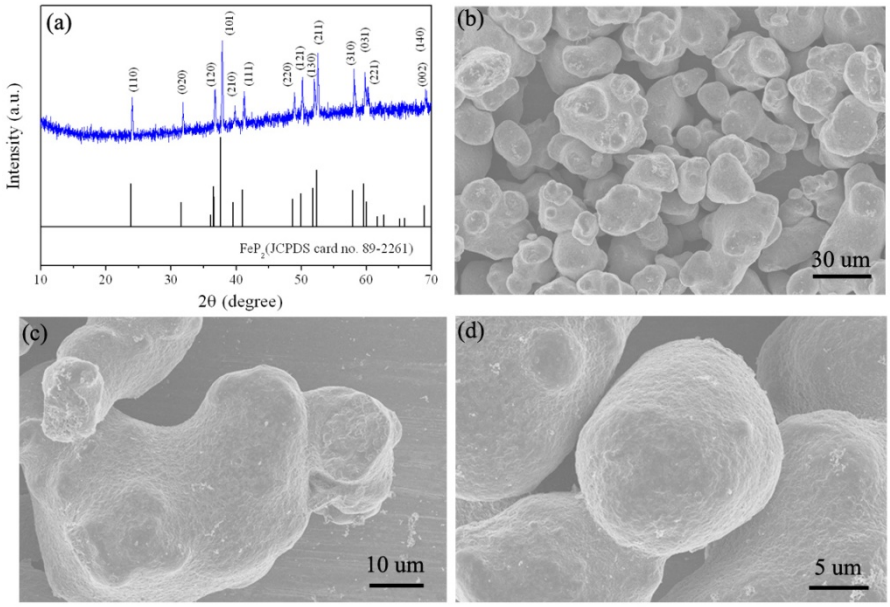

Fig. S3. (a) Powder XRD pattern for the bulk FeP_2 (blue, top) and the standard pattern of FeP_2 (JCPDS card no. 89-2261) (black, bottom), (b) low-magnified, (c) and (d) high-magnified SEM images for the as-prepared bulk FeP_2.

5. Calculation of the relative surface areas between bulk FeP_2 and FeP_2/C nanohybrids

According to the report,[S3] the double layer capacitance (C_{dl}) of the electrocatalysts are expected to be linearly proportional to their effective active surface area, which can be measured by cyclic volatammetry (CV) method. However, since the carbon tubes in our hybrids would contribute to the capacitance, we carry out the CV measurements to roughly estimate the relative surface areas between bulk FeP_2 and FeP_2/C nanohybrids. CV measurements are taking in the region of 0.1-0.3 V vs. RHE and the double-layer capacitance is estimated by plotting the ΔJ (Ja-Jc) at 0.2 V vs. RHE against the scan rate, where the slope is twice C_{dl}.

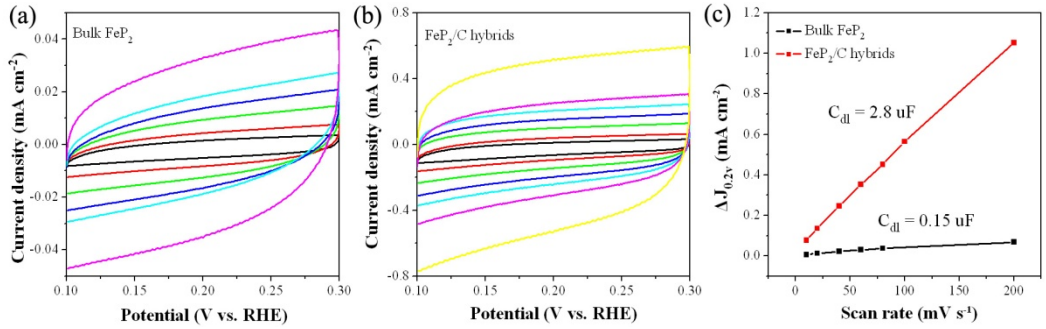

Fig. S4. Cyclic voltammograms in the region of 0.1−0.3 V vs. RHE for (a) the bulk FeP_2 and (b) the FeP_2/C nanohybrids, and (c) the differences in current density (ΔJ = Ja-Jc) at 0.2 V vs. RHE plotted against scan rate fitted to a linear regression allows for the estimation of C_{dl}. The current density in the figures is based on the geometric surface areas of the glassy carbon electrodes.

6. Calculation of the electroactive surface area of Pt/C electrode

The electroactive surface area of Pt/C electrode is evaluated by measuring the charge collected in the H adsorption/desorption region after double-layer correction and assuming a value of 220 mC cm^{-2} for the adsorption of a hydrogen monolayer,[S4] and according to the following equation: $S = Q_H/Q_S$, the electroactive surface area of the Pt/C electrode can be determined to be 4.30 cm^{-2}, and the real roughness factor of the Pt/C electrode is 60.9.

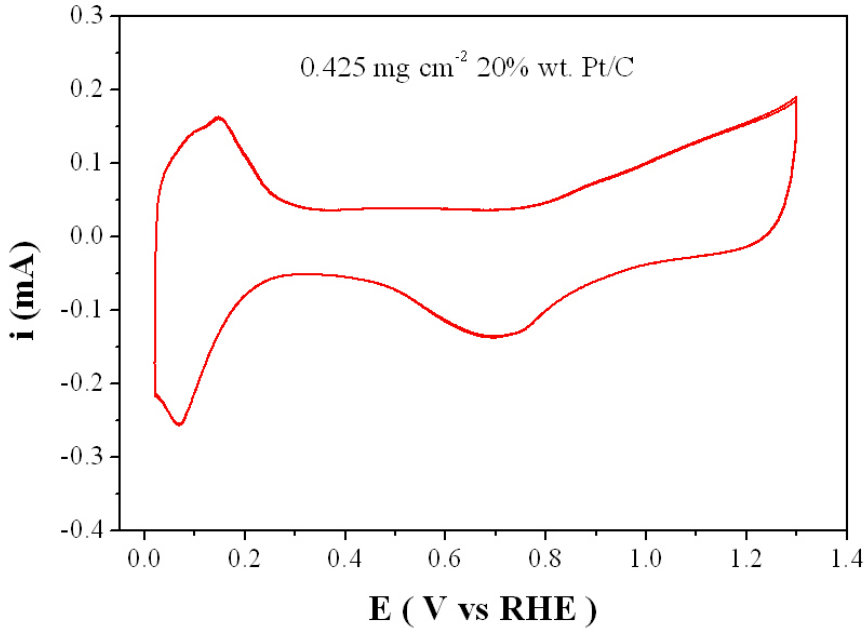

Fig. S5. CV of the Pt/C electrode (20% wt.) with catalysts loading of 0.425 mg cm^{-2} measured in 0.50 M H_2SO_4 aqueous solution and the scan rate = 20 mV s^{-1}. The electroactive surface area is determined from the characteristic peak in the negative region (from 0.05 to 0.40 V vs. RHE) attributable to atomic hydrogen

adsorption on the Pt particles surfaces.

7. Density functional theory (DFT) calculations on the Gibbs free energies for hydrogen adsorption on FeP_2 (120) facet with P terminated surface

All the calculations are performed using density-functional theory (DFT) method as implemented in a Vienna *ab initio* simulation package (VASP)[S5-S7] by using generalized gradient approximation Perdew-Burke-Eznerhof (GGA-PBE) method.[S8] Projector augmented wave method (PAW)[S9,S10] is used to describe the interaction between the atomic cores and the electrons. The (1 × 1) surface of FeP_2 (120) is chosen for the consideration of the dominating planes based on experimental observation, which is simulated by using a four-atom-layer-thick slab. In our calculations, the Brillouin zone of the slab is sampled by the 10 × 2 × 1 Monkhorst-Pack k-points. As the P-terminated surface is identified as the active sites for adsorption/desorption of H in the case of MoP system,[S11] we only consider the P terminated surface of the FeP_2 for the calculation in the current work.

Adsorption of H atom(s) on FeP_2 (120) surface

The differential adsorption energy of H adsorption is chosen to describe the stability of hydrogen according to the literature,[S12] which is given below:

$$\Delta E_H = E(FeP_2 + nH) - E(FeP_2 + (n\text{-}1)\,H) - 1/2\,E(H_2), \qquad (1)$$

where $E(FeP_2 + nH)$ is the total energy of FeP_2 with the n hydrogen atoms adsorbed on surface, $E(FeP_2 + (n\text{-}1)H)$ is the total energy of FeP_2 with (n-1) hydrogen atoms adsorbed on surface and $E(H_2)$ is the total energy of hydrogen molecule in gas phase. Since top surface in our model has four P atoms, adsorption of one, two, three or four H atoms just corresponds to the H coverage of 25%, 50%, 75% or 100% on the surface.

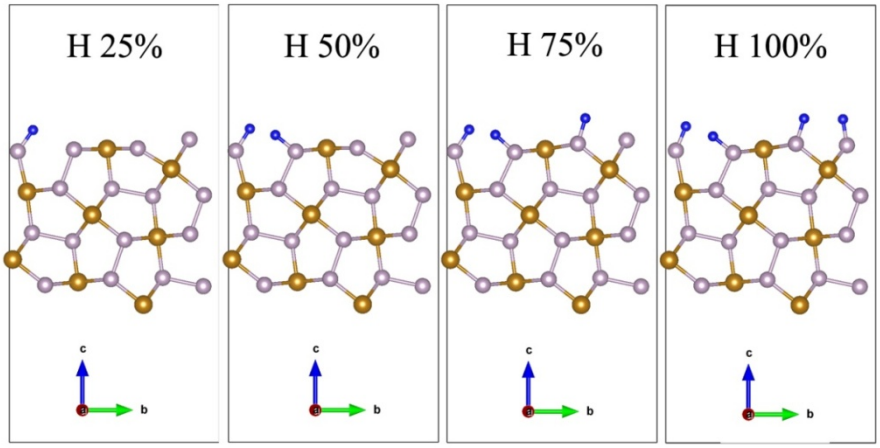

Fig. S6. H adsorbed FeP_2 (120) with P terminated surfaces. (Fe—brown sphere, P—purple sphere, H—blue sphere).

Catalytic activity of FeP_2

To evaluate the catalytic activity of FeP_2, we calculate the Gibbs free energy of hydrogen adsorption as below:

$$\Delta G°_H = \Delta E_H + \Delta E_{ZPE} - T\,\Delta S_H \quad (2)$$

where ΔE_{ZPE} is the difference in zero point energy between the adsorbed state and the gas phase, ΔS_H is the entropy difference between the adsorbed state and the gas phase. The gas phase entropy of H is taken from ref. S13. The calculated $\Delta G°_H$ values for H adsorption on FeP_2 (120) with P terminated surface are listed in Table S2. It will be a good catalyst for hydrogen evolution if the free energy of adsorbed H is close to that of the reactant or product (*i.e.*, $\Delta G°_H \approx 0$). From the DFT results, we can obtain that all of the exposed P atoms on the FeP_2 (120) surface are effective sites for HER, which is responsible for the excellent catalytic activity of FeP_2 in the experiments.

Table S1. Calculated binding energy and Gibbs free energy of H adsorption on FeP_2 (120) with P terminated surface.

H Coverage	ΔE_H (eV)	$\Delta G°_H$ (eV)
25%	-0.286	-0.03
50%	-0.195	0.06
75%	-0.336	-0.08
100%	-0.206	0.05

8. The cycling stability of the FeP_2/C nanohybrids in 0.50 M H_2SO_4

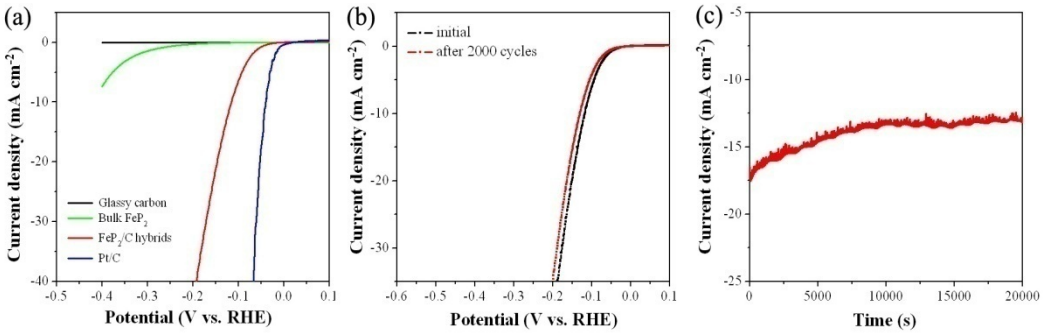

Fig. S7. (a) Polarization curves of the FeP_2/C nanohybrids, bulk FeP_2, bare glassy carbon and Pt/C electrode in 0.50 M H_2SO_4 with a scan rate of 5 mV s^{-1}, (b) polarization curves of the FeP_2/C nanohybrids initially and after 2000 CV scans between +0.2 and −0.2 V vs. RHE, and (c) time-dependent current density curve for the FeP_2/C nanohybrids under static overpotential of 150 mV for 20000 s. The current density in the figures is based on the geometric surface areas of the glassy carbon electrodes.

9. Synthesis of $FeSe_2$/C hybrids with XRD pattern, SEM and TEM images

Synthesis of $FeSe_2$/C hybrids. $Fe(C_5H_5)_2$ (0.4 mmol, 0.0744g) and Se powder (0.8 mmol, 0.0632g) are tableted and put into a quartz tube (φ8 mm × 150 mm), which is then evacuated and sealed. Then, the tube is loaded into a resistance furnace horizontally, heated from room temperature to 600 °C at a rate of 2 °C /min, and kept at this reaction temperature for 20 h. After the tube is naturally cooled to room temperature, the products are collected.

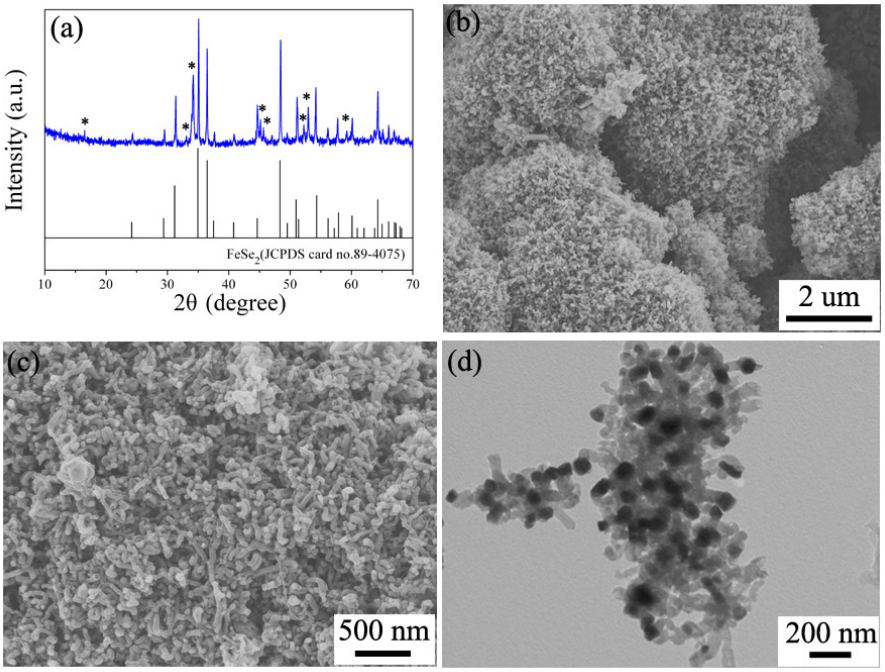

Fig. S8. (a) Powder XRD pattern for the $FeSe_2$/C hybrids (blue, top) and the standard pattern of $FeSe_2$ (JCPDS card no. 89-4075) (black, bottom). The peaks marked with (*) are indexed to Fe_3Se_4 (JCPDS card no. 71-2251), (b) low-magnified, (c) high-magnified SEM images, and (d) TEM image for the as-prepared $FeSe_2$/C hybrids.

Supplementary references

S1. J. Wang, Q. Yang and Z. Zhang, *J. Phys. Chem. Lett.*, 2009, **1**, 102–106.

S2. S. Boyanov, D. Zitoun, M. Ménétrier, J. C. Jumas, M. Womes and L. Monconduit, *J. Phys. Chem. C,* 2009, **113**, 21441−21452.

S3. M. A. Lukowski, A. S. Daniel, F. Meng, A. Forticaux, L. Li and S. Jin, *J. Am. Chem. Soc.*, 2013, **135**, 10274–10277.

S4. D. Chen, Q. Tao, L. W. Liao, S. X. Liu, Y. X. Chen and S. Ye, *Electrocatalysis*, 2011, **2**, 207–219.

S5. G. Kresse, and J. Furthmüller, *Phys. Rev. B,* 1996, **54**, 11169−11186.

S6. G. Kresse and J. Hafner, *Phys. Rev. B,* 1993, **48**, 13115−13118.

S7. G. Kresse and J. Furthmüller, *Comput. Mater. Sci.,* 1996, **6**, 15−50.

S8. J. P. Perdew, K. Burke and M. Ernzerhof, *Phys. Rev. Lett.,* 1996, **77**, 3865−3868.

S9. P. E. Blöchl, *Phys. Rev. B,* 1994, **50**, 17953−17979.
S10. G. Kresse and D. Joubert, *Phys. Rev. B,* 1999, **59**, 1758−1775.
S11. P. Xiao, M. A. Sk, L. Thia, X. Ge, R. J. Lim, J. Y. Wang, K. H. Lim and X. Wang, *Energy Environ. Sci.*, 2014, **7**, 2624–2629.
S12. B. Hinnemann, P. G. Moses, J. Bonde, K. P. Jørgensen, J. H. Nielsen, S. Horch, I. Chorkendorff and J. K. Nørskov, *J. Am. Chem. Soc.,* 2005, **127**, 5308−5309.
S13. P. W. Atkins, *Physical Chemistry*, Oxford University Press, Oxford, 1998.